Supplementary Information

Transparent tissue in solid state for solvent-free and antifade 3D imaging

Fu-Ting Hsiao, Hung-Jen Chien, Ya-Hsien Chou, Shih-Jung Peng, Mei-Hsin Chung, Tzu-Hui Huang, Li-Wen Lo, Chia-Ning Shen, Hsiu-Pi Chang, Chih-Yuan Lee, Chien-Chia Chen, Yung-Ming Jeng, Yu-Wen Tien, and Shiue-Cheng Tang

Index of Supplementary Figures, Tables, and Movies

Supplementary Fig. 1

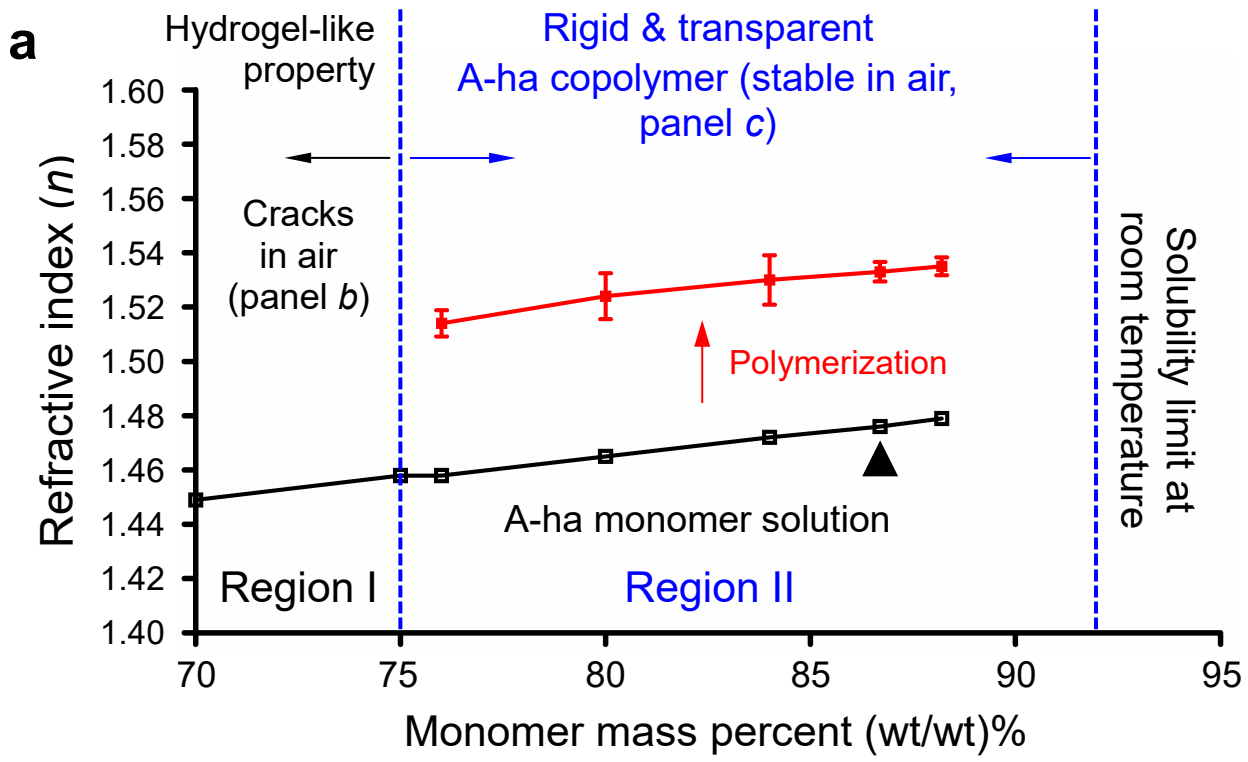

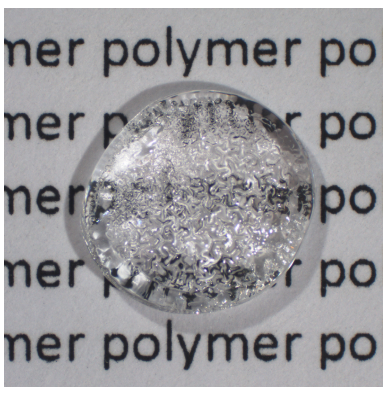

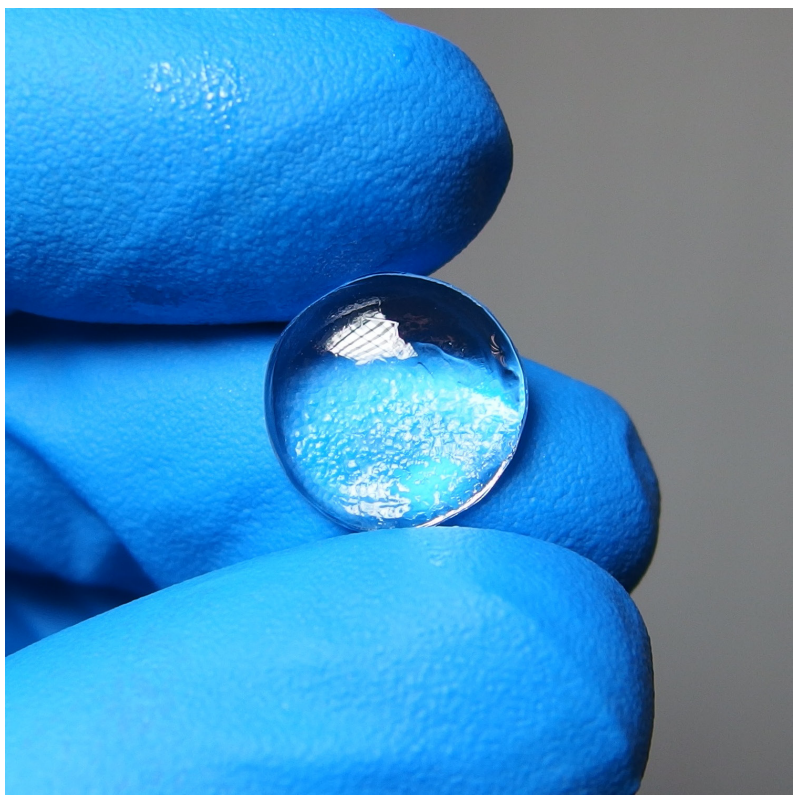

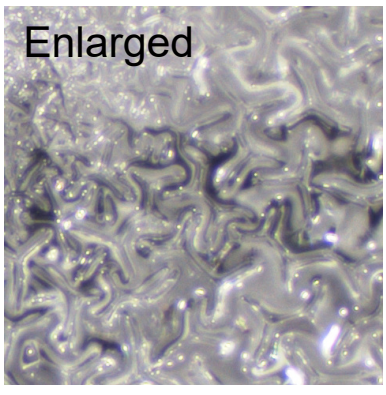

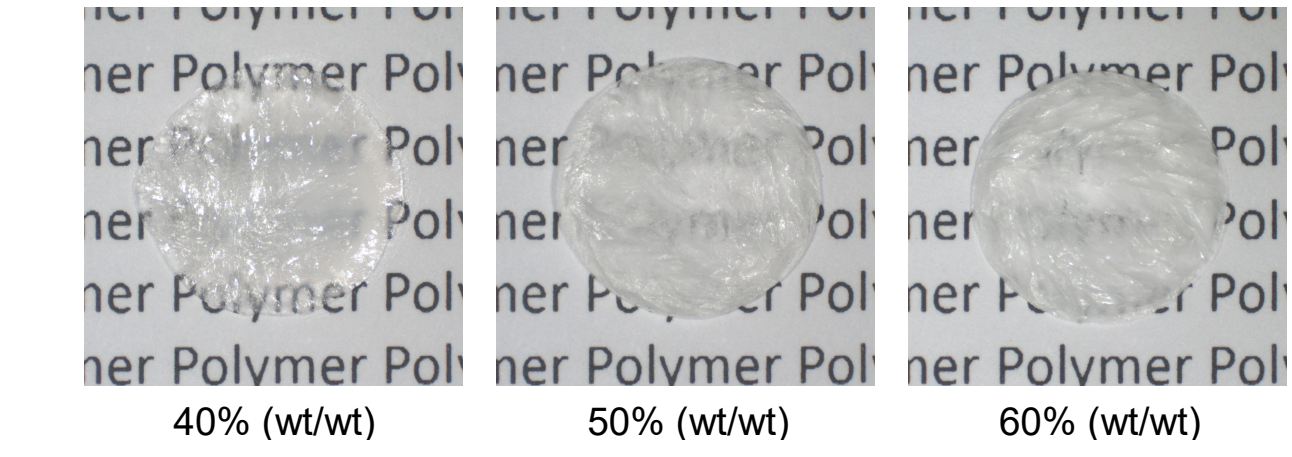

Supplementary Figure 1 (related to Fig. 1a, b)**. Gel-like vs. rigid acrylamide-based A-ha copolymer.** Acrylamide and n-hydroxymethyl acrylamide (molar ratio 1:1) were polymerized at low (≤75%, Region I) vs. high (≥76%, Region II) mass fraction (**a**). The former developed cracks in air and became opaque (**b** and **b'**; 75% wt/wt), while the latter stayed rigid and transparent in air and can be stored at room temperature without losing its optical (high-*n*) property (**c**; 86.7% wt/wt, *n*=1.53; 24 independent A-ha syntheses). 6 independent A-ha syntheses at 88.2% wt/wt and 4 independent A-ha syntheses at 84%, 80%, and 76% wt/wt were used to estimate the copolymer refractive indexes. Data are presented as means ± standard deviation. Arrowhead in *a* indicates the monomer mass fraction (86.7% wt/wt) used in routine A-ha copolymer synthesis. (**d**) Opaque polyacrylamide homopolymer in air (photo-polymerized at 40%, 50%, and 60% wt/wt). Acrylamide reaches solubility limit at 60% wt/wt in water at room temperature.

Supplementary Fig. 2

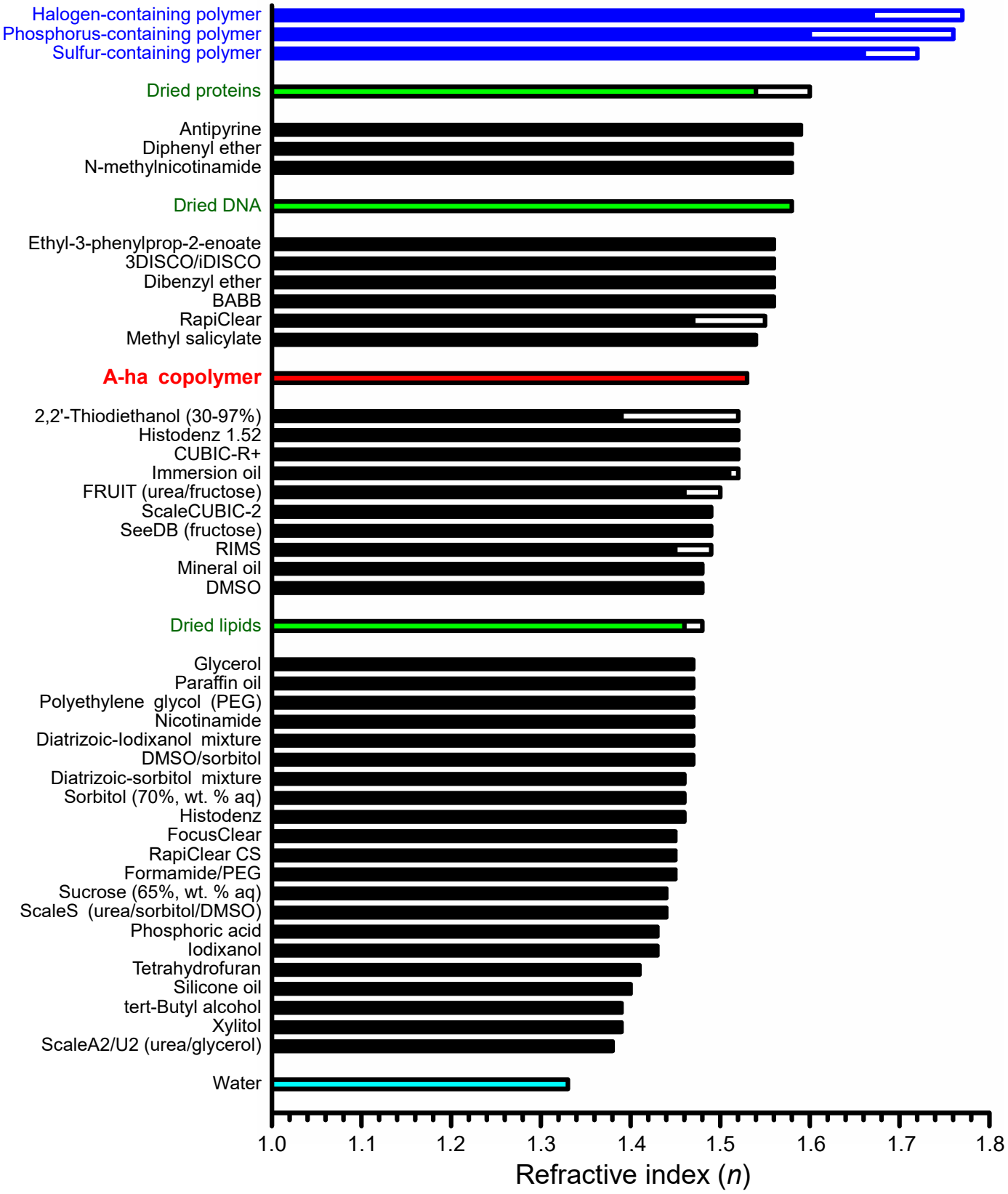

Supplementary Figure 2 (related to Fig. 2)**. Comparison of refractive indexes among high-*n* polymers, cellular components** (proteins, DNA, and lipids)**, and tissue-clearing reagents.** Empty bar indicates the range of refractive indexes of a polymer, cellular component, or reagent[1-7,17,29-31].

Supplementary Fig. 3

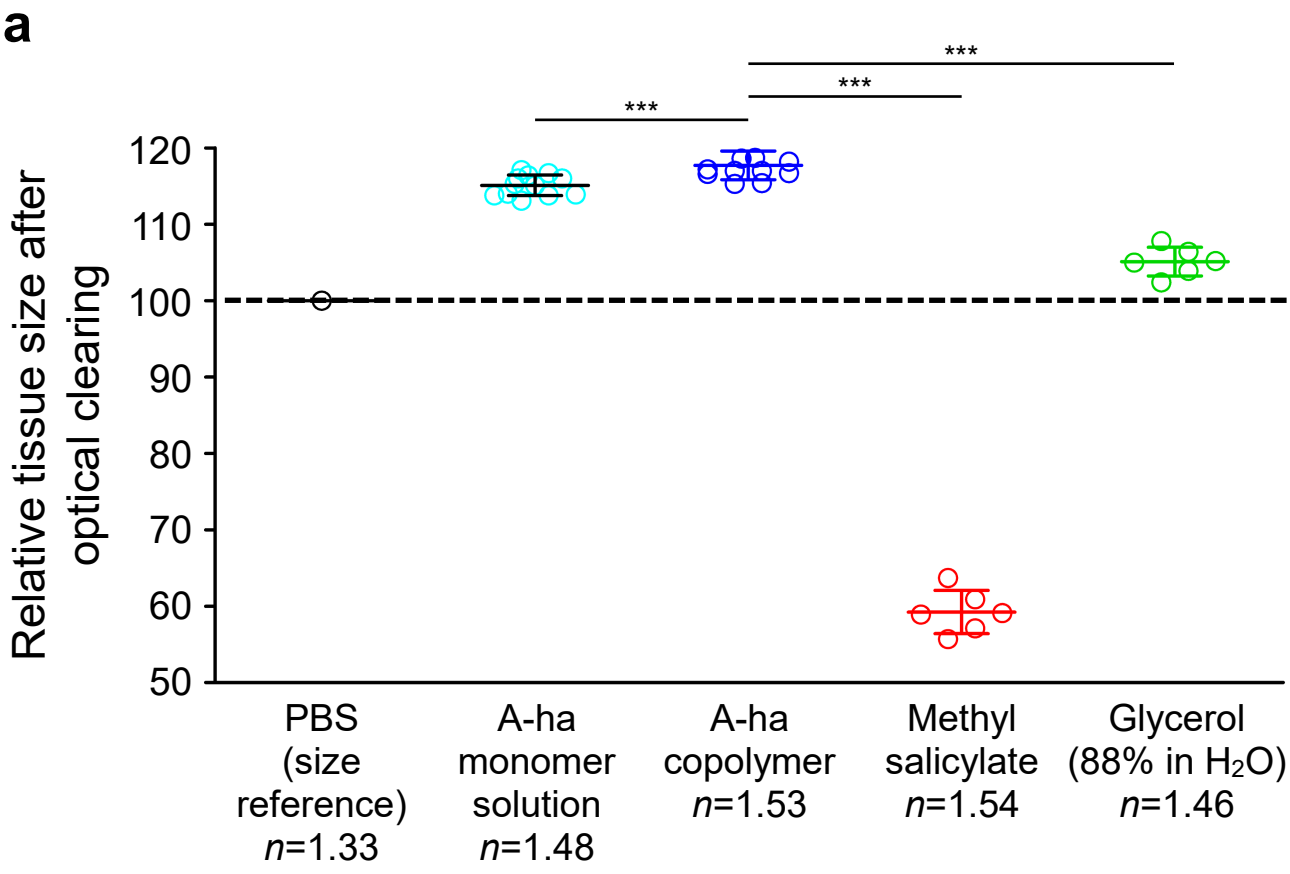

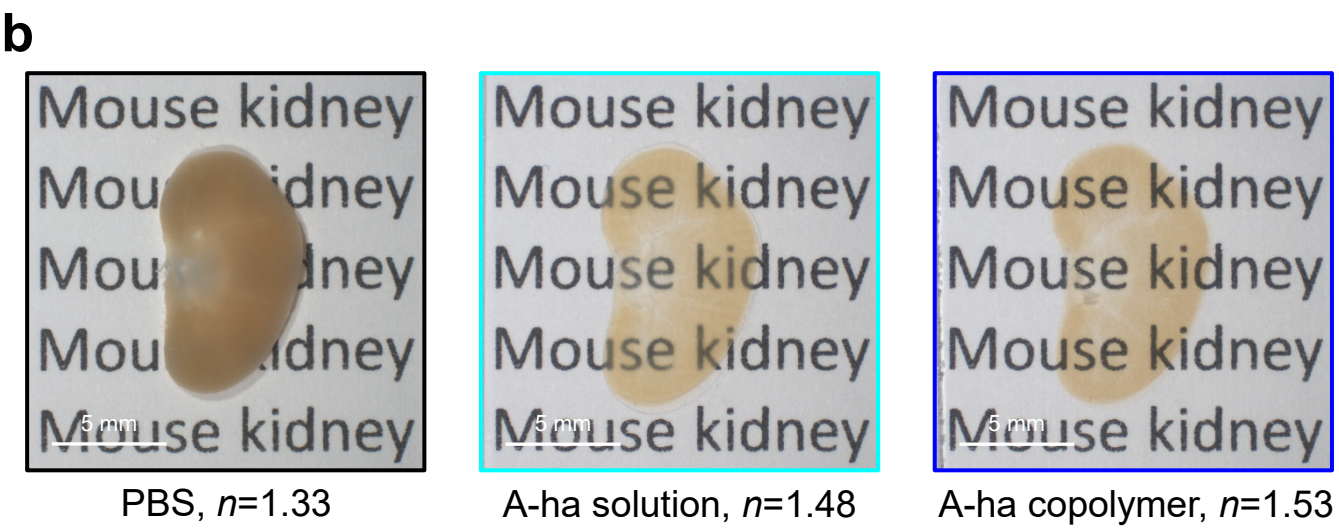

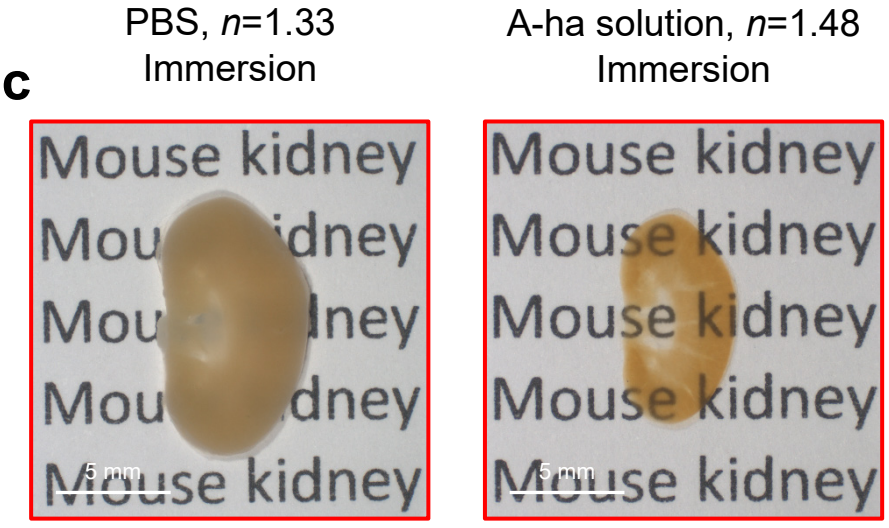

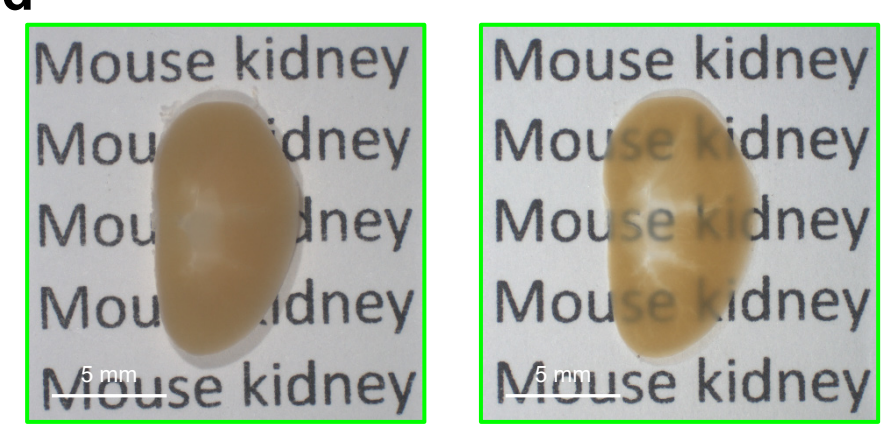

Supplementary Figure 3 (related to Fig. 3b-g)**. Mild tissue expansion of A-ha-based clearing.** (**a**) Tissue expansion or shrinkage after immersed/embedded in high-*n* media for optical clearing. Pixels of mouse kidney were used to estimate the change. Expressed as % of kidney in PBS. Twelve independent A-ha immersions/embeddings and six independent methyl salicylate and glycerol immersions were performed for the quantitative measurement. ***p<0.001 vs. tissue in A-ha copolymer (two-sided unpaired Student's t-test). Data are presented as means ± standard deviation. (**b-d**) Representative images of A-ha, methyl salicylate, and glycerol-based optical clearing of mouse kidney (500 µm in thickness). **(e)** Quantitative measurement of tissue size via stereomicroscopy. The kidney specimen was first immersed in PBS (between coverslips with a 500-µm spacer) and then imaged via stereomicroscopy (Carl Zeiss, SteREO Discovery.V12) to record the pixels occupied by the tissue (defined as 100). Afterward, the tissue was cleared in the A-ha copolymer (or clearing liquid) and then imaged again under the same microscope. The number of pixels recorded in the clearing condition was divided by that in PBS to estimate the relative tissue size after optical clearing (y axis of panel *a*). In the process, the same background "Mouse kidney" was placed under the specimen to serve as the size standard (relative to tissue) and to demonstrate the change in tissue transparency.

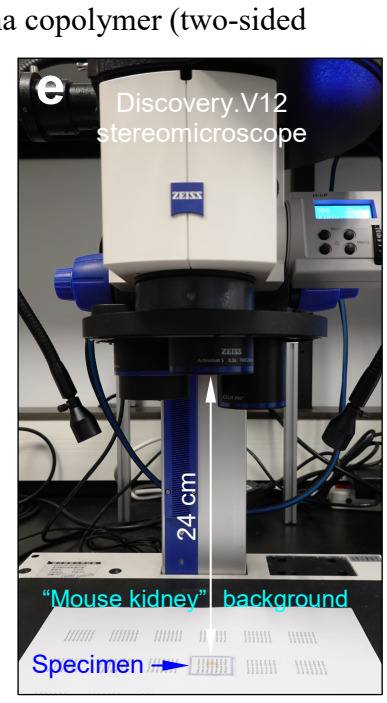

Supplementary Fig. 4

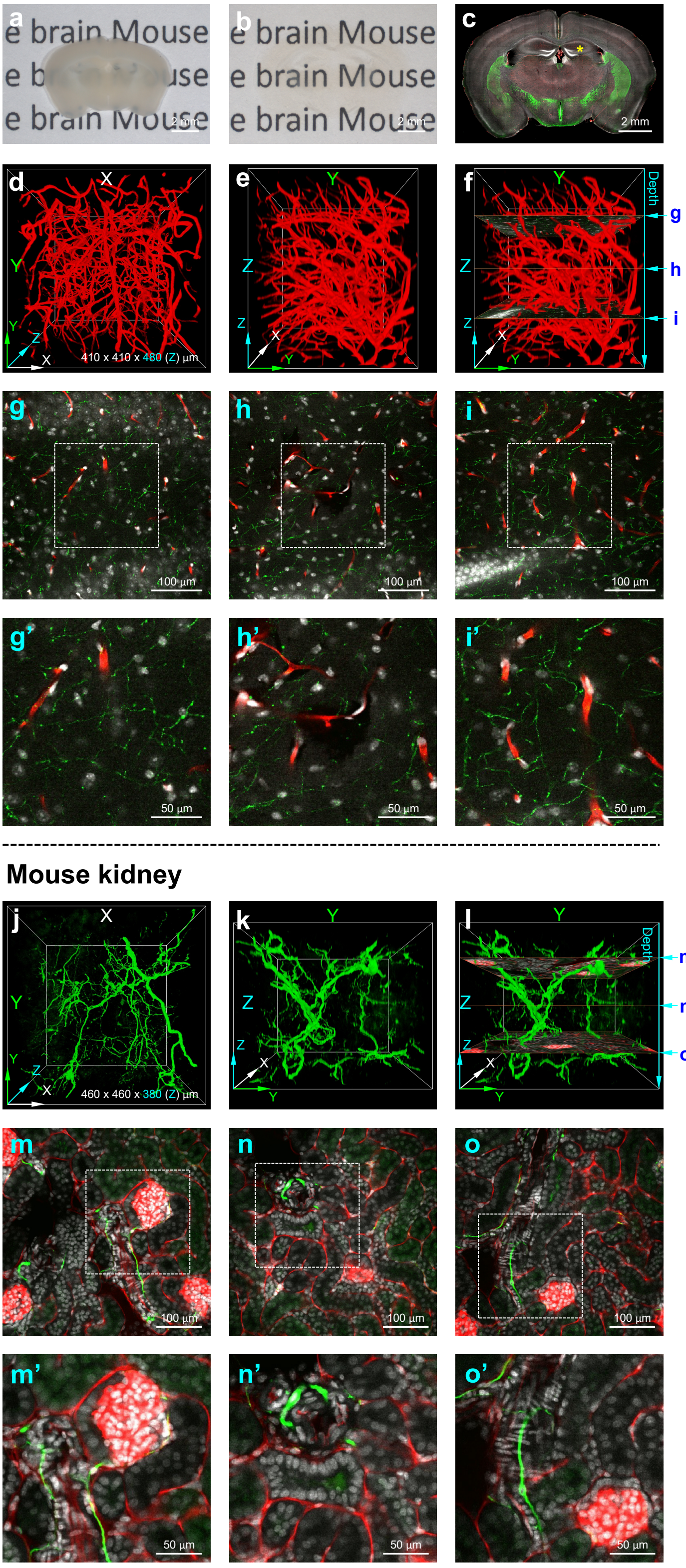

Supplementary Figure 4 (related to Fig. 4)**. Tissue clearing and in-depth mouse brain and kidney imaging in A-ha copolymer.** (**a, b**) Opaque vibratome section of mouse brain in PBS (~500 µm in thickness) vs. in A-ha copolymer (transparent). (**c**) Fluorescence tissue map of mouse brain in A-ha copolymer. *a-c* examine the same brain. Green, tyrosine hydroxylase (TH) staining; red, perfusion labeling of blood vessels; white, DAPI. Asterisk indicates the hippocampal area examined in *d-f* (3D projection) and *g-i* (2D image). (**d-f**) 3D vascular projection. *d* and *e* are projections from the XY and YZ planes, respectively. Z, imaging depth. In *f*, depths at 110, 240, and 360 µm along focal depth (Z axis) are labeled and their XY images are presented in *g*, *h*, and *i*, respectively. (**g-i**) In-depth images of TH^+ nerve fibers. Boxes in *g-i* are enlarged in *g'-i'*. **(j-o)** 3D projection and 2D image of mouse kidney innervation. The kidney is optically cleared in the A-ha copolymer as presented in **Fig. 3f**. Green, tubulin beta 3 (TUBB3, Biolegend, #657402) staining of nerves; red, perfusion labeling of blood vessels; white, DAPI. *j* and *k* are projections from the XY and YZ planes, respectively. In *l*, depths at 80, 190, and 300 µm along focal depth (Z axis) are labeled and their XY images are presented in *m*, *n*, and *o*, respectively. Boxes in *m-o* are enlarged in *m'*-o*'*. Panel *a-i* and *j-o* are derived from two independent tests of mouse brain and kidney labeling, A-ha embedding, and 3D imaging. **Supplementary Movie 3** and **4** show the in-depth recordings of neurovascular signals in *d-i* (hippocampus, TH^+) and *j-o* (innervation of glomeruli, $TUBB3^+$), respectively.

Supplementary Fig. 5

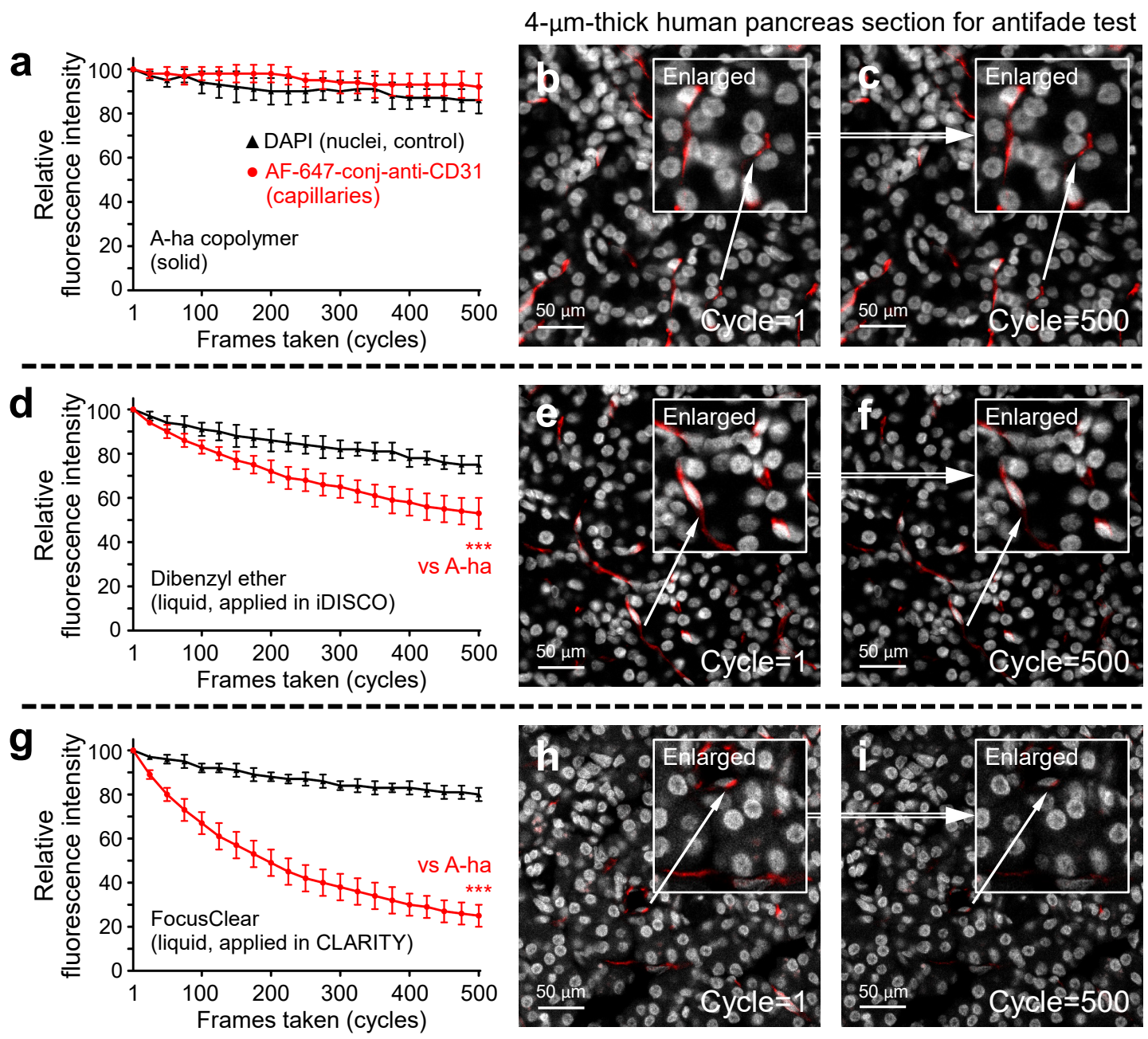

Supplementary Figure 5 (related to Fig. 6a-c)**.** (**a-l**) Comparison of Alexa Fluor (AF) -647 stability in A-ha (***a-c***) vs. the immersion liquids applied in iDISCO (dibenzyl ether, ***d-f***; organic), CLARITY (FocusClear, ***g-i***; aqueous), and CUBIC (sucrose/urea/triethanolamine solution, ***j-l***; mixture) -based clearing methods. *b-c*, *e-f*, *h-i*, and *k-l*, are representative images. Also see **Supplementary Movie 9** for side-by-side and frame-by-frame comparison of the four conditions. Human pancreas was labeled with DAPI (white, stable control) and anti-CD31 (red, AF-647-conjugated primary antibody; direct immunohistochemistry, indicator). The 500-frame antifade test was performed on the 4-µm microtome section of human pancreas; thus, only the chemical environment, not tissue clearing efficiency, affects the fluorescence detection. On average, the AF-647 signals decreased by 8±6%, 47±7%, 75±5%, and 53±3% in the A-ha copolymer and the solutions of dibenzyl ether, FocusClear, and sucrose/urea/triethanolamine, respectively (n=6 independent antifade tests). Data are expressed as % of fluorescence intensity at cycle=1 (means with standard deviation). ***p<0.001, vs. A-ha (two-sided unpaired Student's t-test). (**m, n**) Stability of nuclear dyes when embedded in A-ha copolymer or immersed in Ce3D clearing liquid. DAPI, Hoechst 33342 (Thermo #H3570), and propidium iodide (PI, Thermo #P21493) show 14±6%, 11±3%, and 7±7% decreases in fluorescence intensity in the A-ha copolymer (4-µm human pancreas section as in ***a-l***), respectively, after 500 frames were taken from the labeled nuclei. In the aqueous Ce3D clearing solution (***n***), the same DAPI, Hoechst, and PI show 12±2% (p=0.42, nonsignificant vs. A-ha), 10±4% (p=0.53, nonsignificant vs. A-ha), and 18±6% (*p<0.05, vs. A-ha) decreases in fluorescence intensity, respectively (n=6 independent antifade tests; two-sided unpaired Student's t-test). Data are presented as means with standard deviation. In the six conditions (***m, n***), the decreases are all less than 20% in the 500-frame antifade test, indicating the intrinsic stability of the three DNA intercalating/binding agents in fluorescence imaging.

Supplementary Fig. 6

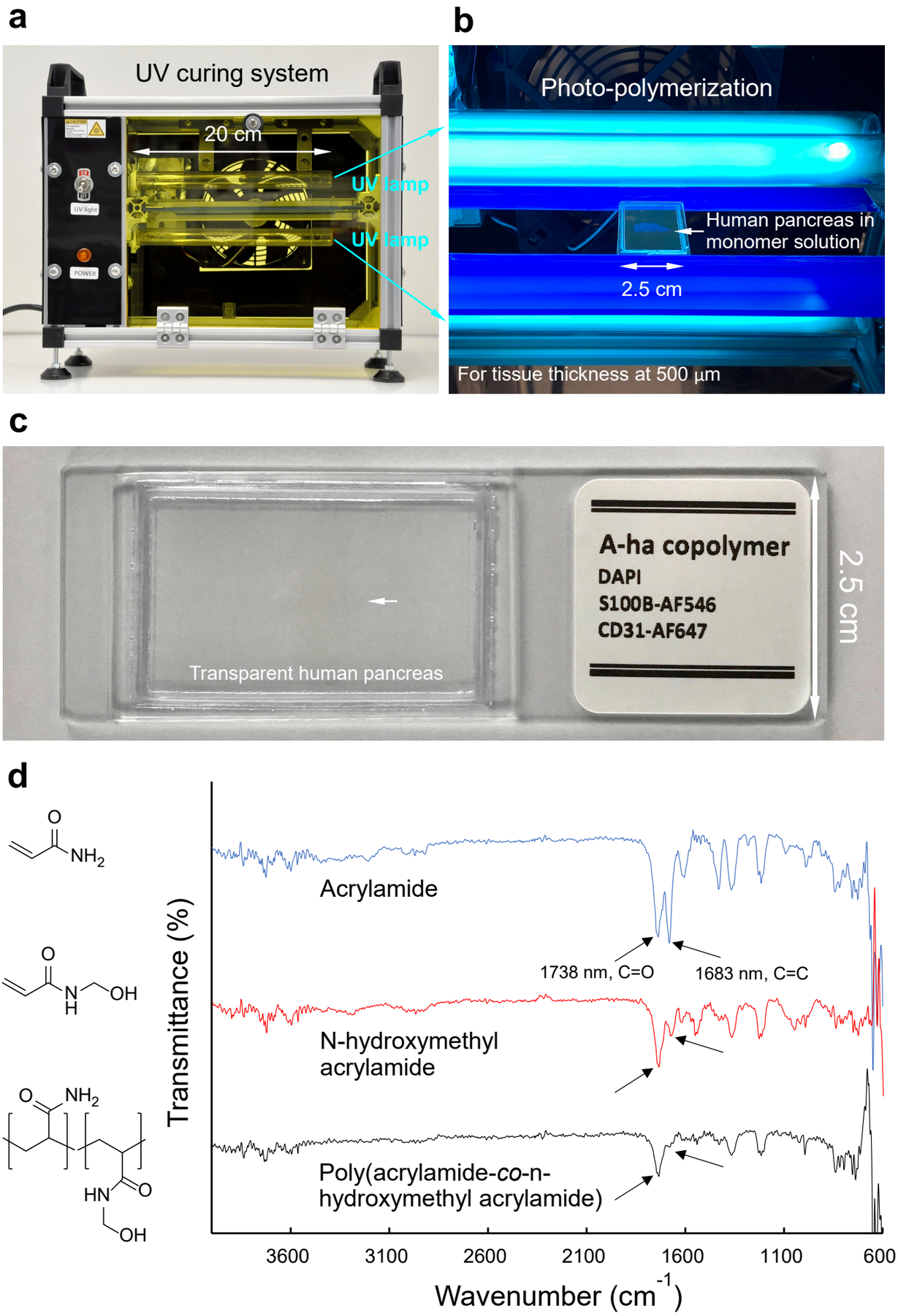

Supplementary Figure 6 (related to Methods)**. Photo-polymerization and FT-IR analysis of A-ha copolymer. (a, b)** UV curing system and photo-polymerization. Two pairs of UV lamps (Philips TUV PL-L 18W/4P; emission peak at 253.7 nm) were placed at the top and bottom of the specimen for irradiation (irradiance: 9.6 mW/cm^2). Tissue (human pancreas) sandwiched between two coverslips via an iSpacer (SunJin Lab) was immersed in the monomer solution with Irgacure 2959 photoinitiator (0.04% mass fraction) to facilitate photo-polymerization. **(c)** Transparent human pancreas in A-ha copolymer on standard microscope slide. The fluorescent labeling is antifade and ready for 3D confocal and/or super-resolution imaging. **(d)** FT-IR spectra of reactants (acrylamide and n-hydroxymethyl acrylamide) and product (A-ha copolymer) following the photo-polymerization. After the reaction, a weak or absent absorption peak at 1683 cm^{-1} (alkenes) indicates that the monomers of acrylamide and n-hydroxymethyl acrylamide were polymerized and changed to poly(**a**crylamide-*co*-n-**h**ydroxymethyl **a**crylamide), the A-ha copolymer.

Supplementary Fig. 7

a Acquisition parameters for in-depth Airyscan of human pancreas (40x objective)

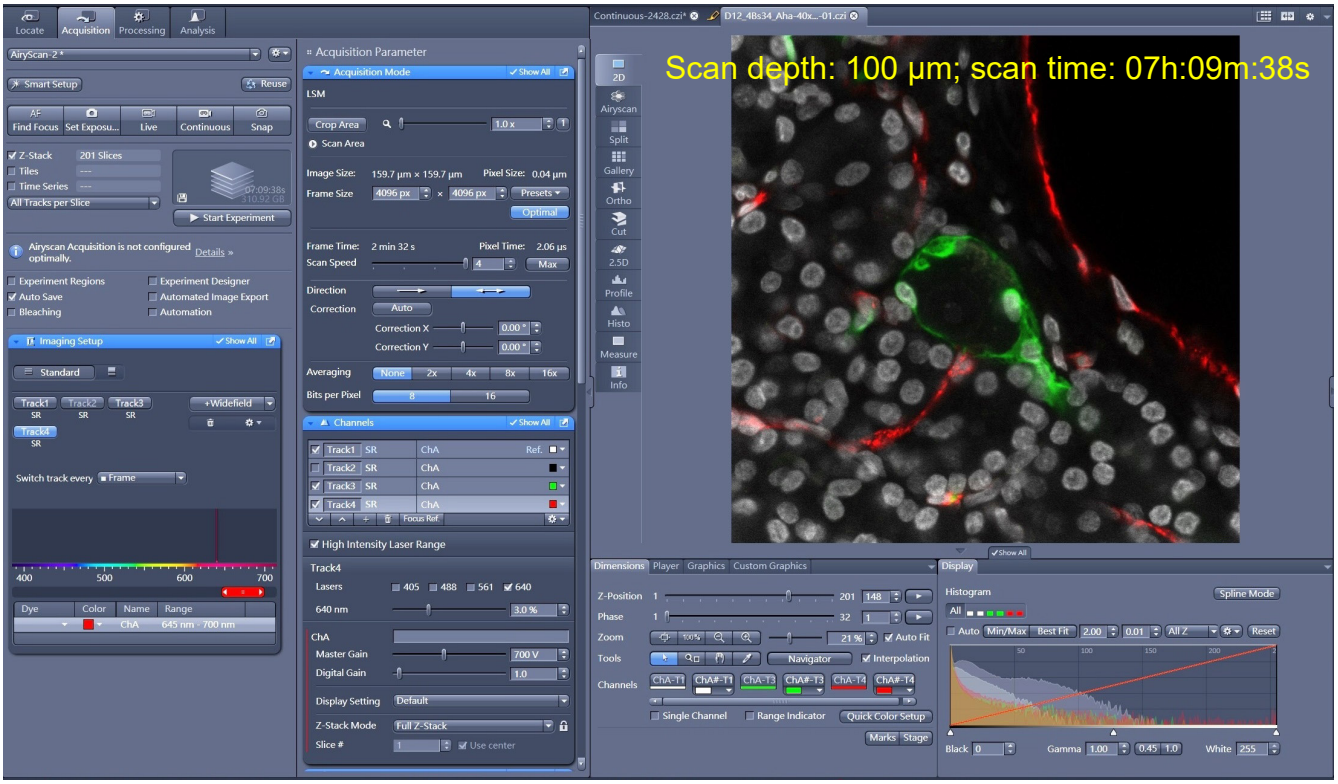

b Acquisition parameters for in-depth Airyscan of human pancreas (63x objective)

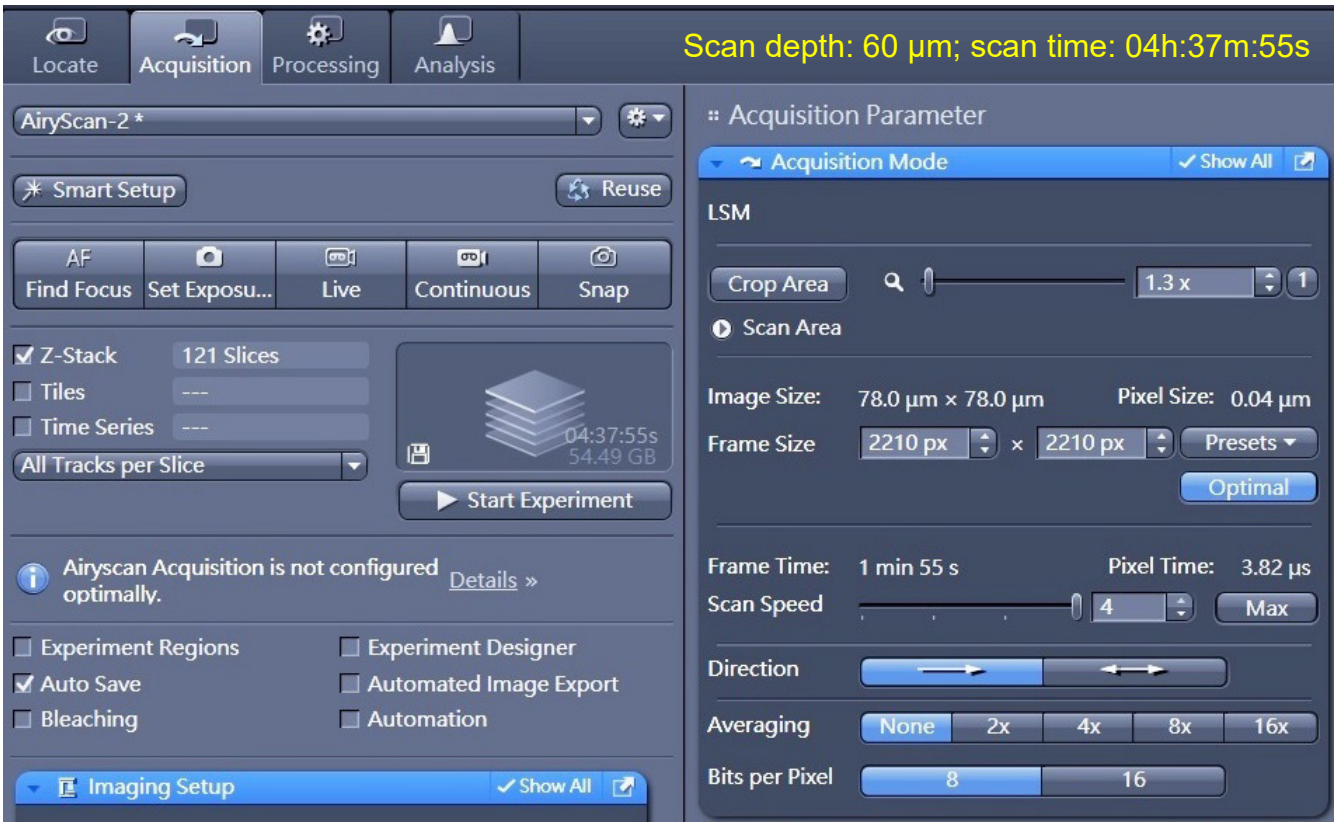

Supplementary Figure 7 (related to Methods)**. Acquisition parameters for in-depth Airyscan of A-ha embedded human pancreas.** Two types of oil-immersion objective, Plan-Apochromat 40x/1.3 Oil DIC (**a**) and Plan-Apochromat 63x/1.4 Oil DIC (**b**) (Carl Zeiss), were sequentially applied to acquire the images presented in **Fig. 7** and **Supplementary Movie 10**.

Supplementary Table 1

Summary of primary antibodies used in illustrations.

Illustration		Primary antibody (category number)	Dilution	Color code
Figure 4	panel c-j	tyrosine hydroxylase (AB152)	1: 100	Green
Figure 5	panel c, e-j	S100B (ab52642)	1: 100	Green
		AF-647-conjugated anti-CD31 (ab215912)	1: 100	Red
Figure 5	panel k-o	glucagon (ab10988)	1: 100	Magenta
		AF-488-cojugated anti-insulin (sc-8033_AF488)	1: 100	Blue
		CK7 (ab68459)	1: 100	Green
Figure 6	panel a-b, d-e, g-h	S100B (ab52642)	1: 100	Green
		AF-647-conjugated anti-CD31 (ab215912)	1: 100	Red
Figure 7	panel b-g	S100B (ab52642)	1: 100	Green
		AF-647-conjugated anti-CD31 (ab215912)	1: 100	Red
Suppl. Fig. 4	panel c-i	tyrosine hydroxylase (AB152)	1: 100	Green
Suppl. Fig. 4	panel j-o	tubulin beta 3 (clone AA10, Biolegend, 657402)	1: 100	Green
Suppl. Fig. 5	panel a-l	AF-647-conjugated anti-CD31 (ab215912)	1: 100	Red
Suppl. Movie 2		tyrosine hydroxylase (AB152)	1: 100	Green
Suppl. Movie 3		tyrosine hydroxylase (AB152)	1: 100	Green
Suppl. Movie 4		tubulin beta 3 (clone AA10, Biolegend, 657402)	1: 100	Green
Suppl. Movie 5		S100B (ab52642)	1: 100	Green
		AF-647-conjugated anti-CD31 (ab215912)	1: 100	Red
Suppl. Movie 6		S100B (ab52642), used in Part 1	1: 100	Green
		AF-647-conjugated anti-CD31 (ab215912)	1: 100	Red
		PGP9.5 (ab108986), used in Part 2	1: 100	Green
Suppl. Movie 7		glucagon (ab10988)	1: 100	Magenta
		AF-488-cojugated anti-insulin (sc-8033_AF488)	1: 100	Blue
		CK7 (ab68459)	1: 100	Green
Suppl. Movie 8		S100B (ab52642)	1: 100	Green
		AF-647-conjugated anti-CD31 (ab215912)	1: 100	Red
Suppl. Movie 9		AF-647-conjugated anti-CD31 (ab215912)	1: 100	Red
Suppl. Movie 10		S100B (ab52642)	1: 100	Green
		AF-647-conjugated anti-CD31 (ab215912)	1: 100	Red
Suppl. Movie 11		S100B (ab52642)	1: 100	Green
		AF-647-conjugated anti-CD31 (ab215912)	1: 100	Red
Suppl. Movie 12		S100B (ab52642)	1: 100	Cyan
		AF-647-conjugated anti-PGP9.5 (ab196173)	1: 100	Green

Note: tyrosine hydroxylase (sympathetic marker), S100B (glial marker), CD31 (endothelial marker), glucagon (islet α-cell marker), insulin (islet β-cell marker), CK7 (epithelial marker), tubulin beta 3 (neuronal marker), and PGP9.5 (neuronal marker).

Supplementary Table 2

Summary of color codes presented in illustrations.

Illustration		Magenta/Red	Green	Blue/Cyan	White
Figure 4	panel a, b (stereomicroscopic image)				
	panel c-j	perfusion labeling of blood vessels	TH		nuclei
Figure 5	panel b (stereomicroscopic image)				
	panel c, e-j	CD31 (blood vessels)	S100B		nuclei
	panel d (H&E image)				
	panel k-o	glucagon	CK7	insulin	nuclei
Figure 6	panel a-b, d-e, g-h	CD31 (blood vessels)	S100B		nuclei
Figure 7	panel a (stereomicroscopic image)				
	panel b-g	CD31 (blood vessels)	S100B		nuclei
Suppl. Fig. 4	panel c-i	perfusion labeling of blood vessels	TH		nuclei
	panel j-o	perfusion labeling of blood vessels	tubulin beta 3		nuclei
Suppl. Fig. 5	panel b-c, e-f, h-i, k-l	CD31 (blood vessels)			nuclei
Suppl. Movie 2		perfusion labeling of blood vessels	TH		nuclei
Suppl. Movie 3		perfusion labeling of blood vessels	TH		nuclei
Suppl. Movie 4		perfusion labeling of blood vessels	tubulin beta 3		nuclei
Suppl. Movie 5	(H&E, left; fluorescence, right)	CD31 (blood vessels)	S100B		nuclei
Suppl. Movie 6, part 1	(H&E, upper left; fluorescence, right)	CD31 (blood vessels)	S100B		nuclei
Suppl. Movie 6, part 2	(stereomicroscopic image, upper left; fluorescence, right)	CD31 (blood vessels)	PGP9.5		nuclei
Suppl. Movie 7		glucagon	CK7	insulin	nuclei
Suppl. Movie 8		CD31 (blood vessels)	S100B		nuclei
Suppl. Movie 9		CD31 (blood vessels)			nuclei
Suppl. Movie 10		CD31 (blood vessels)	S100B		nuclei
Suppl. Movie 11		CD31 (blood vessels)	S100B		nuclei
Suppl. Movie 12			PGP9.5	S100B	nuclei

Note: TH, tyrosine hydroxylase (sympathetic marker), S100B (glial marker), CD31 (endothelial marker), glucagon (islet α-cell marker), insulin (islet β-cell marker), CK7 (epithelial marker), tubulin beta 3 (neuronal marker), and PGP9.5 (neuronal marker).